A Data-driven Personnel Detection Scheme for Indoor Surveillance using Seismic Sensors

Arun Subramanian[a], Satish G. Iyengar[a], Kishan G. Mehrotra[a], Chilukuri K. Mohan[a], Pramod K. Varshney[a*] and Thyagaraju Damarla[b]

[a]Department of Electrical Engineering and Computer Science, Syracuse University, Syracuse, NY 13244, USA;
[b]Army Research Laboratory, Adelphi, MD 20783, USA

ABSTRACT

This paper describes experiments and analysis of seismic signals in addressing the problem of personnel detection for indoor surveillance. Data was collected using geophones to detect footsteps from walking and running in indoor environments such as hallways. Our analysis of the data shows the significant presence of nonlinearity, when tested using the surrogate data method. This necessitates the need for novel detector designs that are not based on linearity assumptions. We present one such method based on empirical mode decomposition (EMD) and functional data analysis (FDA) and evaluate its applicability on our collected dataset.

Keywords: Indoor surveillance, seismic signal processing, test for nonlinearity, empirical mode decomposition, functional data analysis

1. INTRODUCTION

This paper deals with an important application of distributed sensing, namely, indoor surveillance. Many situations (cleared building scenarios, for instance) require scene monitoring for intrusion detection where the presence of surveillance personnel is not feasible. In such cases, signals from sensors deployed in a surveillance region can be processed to provide reliable inference in the event of a security breach. The sensors may be active or passive or a combination of the two. In this work, we consider a linear array of seismic (geophone) sensors. These are passive vibration sensitive sensors that typically have a good low frequency response and sharp attenuation at higher frequencies. The seismic signal, obtained as a result of human intrusion, is a function of the geophone response to the footsteps of the intruder, and is a zero-mean oscillating signal.

The topic of detecting footsteps using seismic/acoustic sensors is not new. Bland[1] has discussed the use of AR coefficients in designing a footstep detection scheme from acoustic and seismic sensors. Succi et al. have suggested[2] the use of signal kurtosis as a test statistic. Their method is based on the intuition that seismic data corresponding to footsteps would be characterized by a "peaky" probability density function and therefore a higher kurtosis. Their design is parametric, assumes that the test statistic is normally distributed and the observations are IID. Wavelet based feature extraction has also been discussed as an extension to the kurtosis based approach.[3] Dibazar et al. have considered[4] the problem of detecting and classifying perimeter intrusion using geophones. They use a neural network approach to classify vehicular and human intrusion and use footsteps as the signature for human intrusion. A cadence based method for footstep detection has been considered by Houston et al.[5] In a previous paper,[6] Iyengar et al. fuse acoustic and seismic signals for footstep detection. Their work discusses a novel approach for the design of a parametric detector using a CCA-copula based approach.

In this paper, we describe experiments in which an indoor deployment of seismic sensors was used to collect footstep data. We also provide an analysis of this data and propose a novel data-dependent signal processing scheme for the detection of footsteps. One of the key drawbacks of the approaches cited above is that methods and features are used that implicitly assume signal stationarity and linearity. This paper seeks to address these issues in the context of seismic signal processing for personnel detection.

Section 2 describes the details of our experiments. We show that a significant proportion of the seismic data exhibits nonlinearity. This finding is discussed in greater detail in Section 3. That most real signals also exhibit

* Corresponding author. Email: varshney@syr.edu

Unattended Ground, Sea, and Air Sensor Technologies and Applications XI, edited by Edward M. Carapezza, Proc. of SPIE Vol. 7333, 733315 · © 2009 SPIE · CCC code: 0277-786X/09/$18 · doi: 10.1117/12.820237

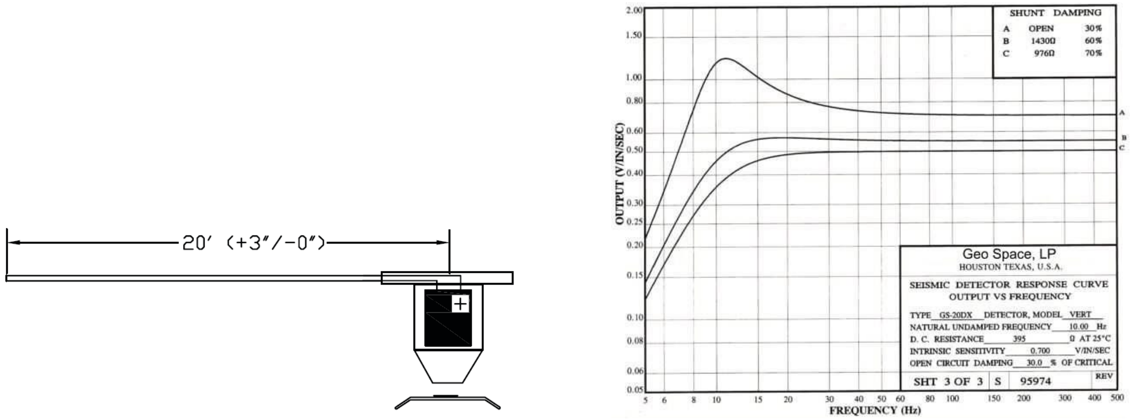

(a) (b)

Figure 1. The GS 20DX geophone. (a) Electrical details. (b) Frequency response curve.

nonstationarity is a well documented fact,[7] and this property is likewise observed in our dataset. We use the nonlinearity and nonstationarity of data as a motivating point for devising a detector based on empirical mode decomposition (EMD). The details of the signal processing are discussed in Section 4. A discussion of the results and concluding remarks are provided in Section 5 and Section 6 respectively.

2. DATA COLLECTION

We conducted experiments at Syracuse University to collect footstep data from geophones. The following subsections discuss the sensor specifications and details of the experiments.

2.1 Sensor description

Six GS 20DX geophones were used for the experiments. The electrical details of a typical sensor[8] are depicted in Figure 1(a) and the frequency response curve is depicted in Figure 1(b). Transduction is achieved by means of a moving coil over a magnetic core. The geophones are designed to be floor mounted. Floor to sensor contact was achieved by means of a coupling bolt screwed to the sensor, which was held to the floor by means of a tripod base. This eliminated the need for structural penetration by means of a probe.

2.2 Experiment description

The six sensors were configured as a linear array. They were placed along the long edge of a hallway. The floor was tiled with thick commercial linoleum. The distance between two adjacent sensors was maintained at 10ft. Data was acquired using a 16 bit A/D converter at a sampling rate of 5kHz. Background data was collected by leaving the sensors in an isolated environment. Footstep data was collected with 20 trials of one person walking and running along the hallway. We, however, restrict our attention to the "background" and "walking" trials. Each "walking" trial lasted approximately 12 seconds. Background data is approximately of a 4 minute duration.

Let i denote the sensor index, i.e., $i = 1, 2, \ldots, 6$. Each sensor observation, $y_i(t)$, is uniformly down-sampled to 1024 Hz. Each $y_i(t)$ is divided into 1 second overlapping frames. Denote by $\mathcal{T}_r$, the set of all time instances contained in the rth frame. Therefore, the cardinality of $\mathcal{T}_r$, $|\mathcal{T}_r|$, is 1024. The inter-frame overlap was set to 50%.

The following sections discuss data analysis and EMD based signal processing for footstep detection.

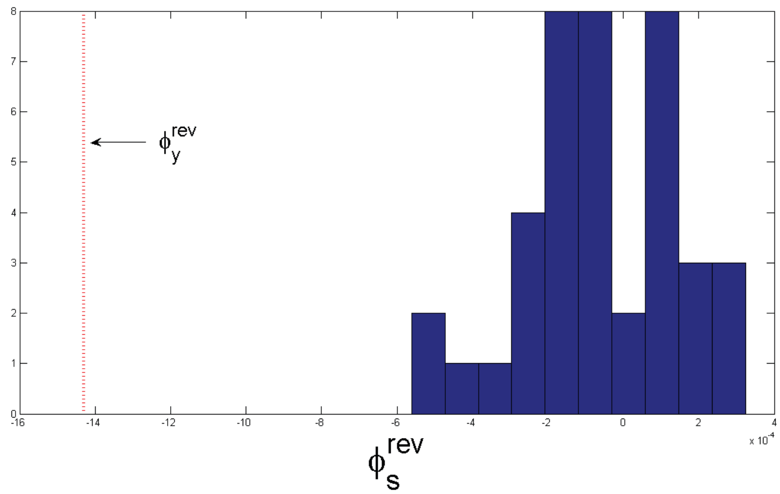

Figure 2. Test for nonlinearity. Histogram is generated using the surrogate data. The statistic of the original time series is represented by the dotted line.

3. TEST FOR NONLINEARITY

A signal $y(t)$ is said to be nonlinear if its current value at $t = t_n$ cannot be predicted or expressed as a linear function of its past values, $t \in [0, t_{n-1}]$. We use the method of surrogate data[9] to analyze the acquired seismic time series for the presence of nonlinearity. The idea is to generate a set of time series (surrogate data set) by resampling from the original measurements so that linear statistical properties of the original data are preserved in the surrogate data set. A nonlinearity measure is then computed for both the surrogate data and the original time series. If the statistics of the measure corresponding to the surrogate and original time series are significantly different, then the null hypothesis that the original time series is a realization of a linear Gaussian process (or monotonic transforms thereof) is rejected.

A third order statistic[9] is used as a signature for nonlinearity in our analysis,

$$\phi^{rev} = \frac{1}{N-1}\sum_{n=2}^{N}(y[n] - y[n-1])^3 \tag{1}$$

where $y[n]$ is the sampled version $y(t)$ and N is the number of samples in the r^{th} frame.

Each frame of $y_i(t)$ (for all i) is tested for the presence of nonlinearity as follows. Forty surrogates $g_k(t)$ $(k = 1, 2, \ldots, 40)$ are generated from a given frame of the original time series $y_i(t)$ using the iterative amplitude adjusted Fourier transform (IAAFT)[9] so that the amplitude spectra of the surrogates matches that of the frame under test while randomizing the phase (uniformly distributed between 0 and 2π). Thus, the surrogates and the original time series have the same linear characteristics and second order properties. The statistic in (1) is then computed for both the surrogates and the test data. For example, consider Fig. 2. The dotted line indicates the value of ϕ_y^{rev}, the statistic computed for sensor data corresponding to a frame from the walking trials. The histogram of ϕ_g^{rev}, computed for the corresponding surrogates is also shown. It is evident that the footstep signal has a nonlinear structure to it as ϕ_y^{rev} does not lie within the distribution of the null hypothesis of linearity. Thus, the null hypothesis can be rejected.

Each frame of the footstep signal is tested for the presence of nonlinearity at 0.05 significance level ($\alpha = 0.05$) using a rank order test proposed by Theiler et al.[10] The case when the frames are two seconds in duration is also considered and results are summarized in Table 1.

4. SIGNAL PROCESSING FOR FOOTSTEP DETECTION

Section 3 discussed the presence of nonlinearity in the seismic data. Nonstationarity can be easily inferred from Fig. 4, which shows sensor measurements for a walking trial. This intuitively suggests that performance

Table 1. Percentage of frames detected as nonlinear

Sensor	*Walking*	
i	*1 second*	*2 second*
1	25	20
2	19	26
3	12	14
4	11	11
5	17	20
6	19	24

improvement in footstep detection may be expected if we account for the nonstationary and nonlinear nature of the data. The popular Fourier and wavelet based techniques make an assumption of linearity. Fourier based time-frequency analysis makes a further assumption of stationarity. In other words, decomposition is achieved by imposing a basis function (the complex exponential for Fourier analysis and the various wavelet kernels) on the data. A better approach would be to allow the data to dictate a decomposition scheme. Empirical mode decomposition (EMD)[11] is a data-driven decomposition technique that has been proposed for analyzing nonlinear and nonstationary data.

We propose an EMD based signal processing scheme for the detection of footsteps. An outline of our proposed system is depicted in Fig. 4. For the detection of pseudo-periodic signals like footsteps, it is of interest to extract "clean" oscillations corresponding to footfalls. EMD is a data-driven decomposition technique that achieves this goal of separating different oscillation modes present in a signal. Fig. 5 and Fig. 6 show the output from the EMD block. It can be seen that the amplitude of oscillations at several scales is captured. However, only a small subset of these modes may characterize the footsteps and thus be of interest. In this paper, we employ a criterion based on the total variation (TV) norm (Section 4.3) to identify this subset. Total variation is a type

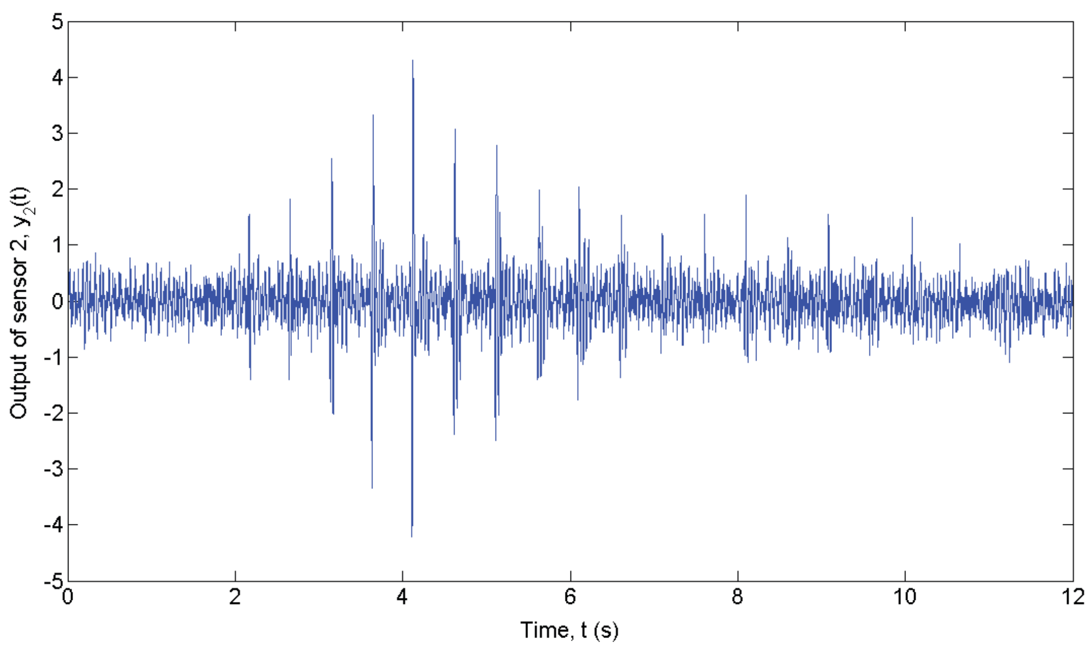

Figure 3. Time series of a footstep trial. Nonstationarity and the impulsive nature of the signal is evident.

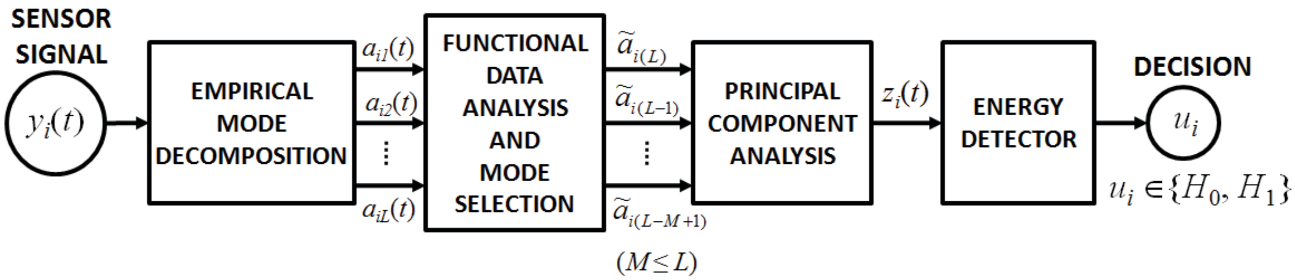

Figure 4. EMD based signal processing scheme for footstep detection for sensor i

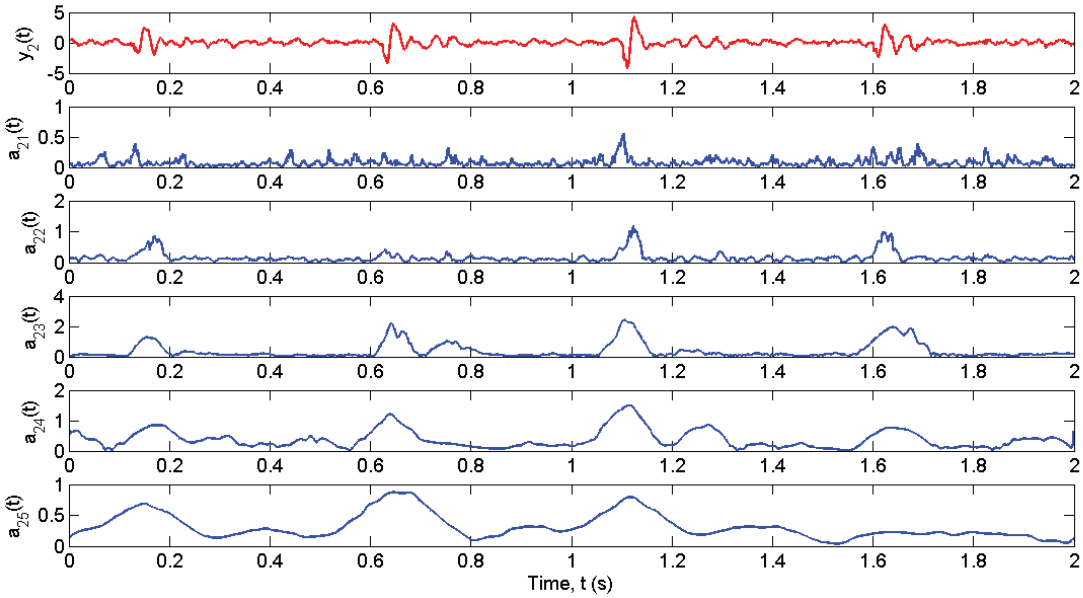

Figure 5. A two second output of the EMD block. The red curve shows the original data. The blue curves represent the amplitude signal of the first five modes. There are a total of 10 modes(for color image see electronic version of manuscript)

of L_1 norm. It provides a local measure of amplitude variation and thus can help extract those modes whose amplitude variations are due to footsteps. However, total variation, and therefore the selection of modes based on it, is sensitive to impulsive background noise. Also, the lack of smoothness in $a_{il}(t)$ (output of the EMD block) can contribute to poor estimates of numerical derivatives necessary for TV computation.

Functional data analysis (FDA) achieves smoothing using derivative based penalization. Ramsay and Silverman[12] discuss methods for analyzing data wherein observations are made from a continuous family of curves. The functional formulation expresses the data as a smooth function of an independent parameter such as time. The specification of "smoothness" as a characteristic of the data implies that one or more derivatives can be reliably estimated. It can be seen from Fig. 7 that the output of the FDA block provides a smoother and thus more reliable footstep envelope. Linear combination of the M modes is achieved using principal components analysis (PCA). We have observed that about 80% of the signal energy is contained in the first principal component score and is the input to the detector – the final block of the system.

The following subsections describe the details of each block.

4.1 Empirical Mode Decomposition

The empirical mode decomposition[11] (EMD) algorithm decomposes a given signal (dataset) into a group of intrinsic mode functions (IMF). The intuition behind defining an intrinsic mode function is that it should capture

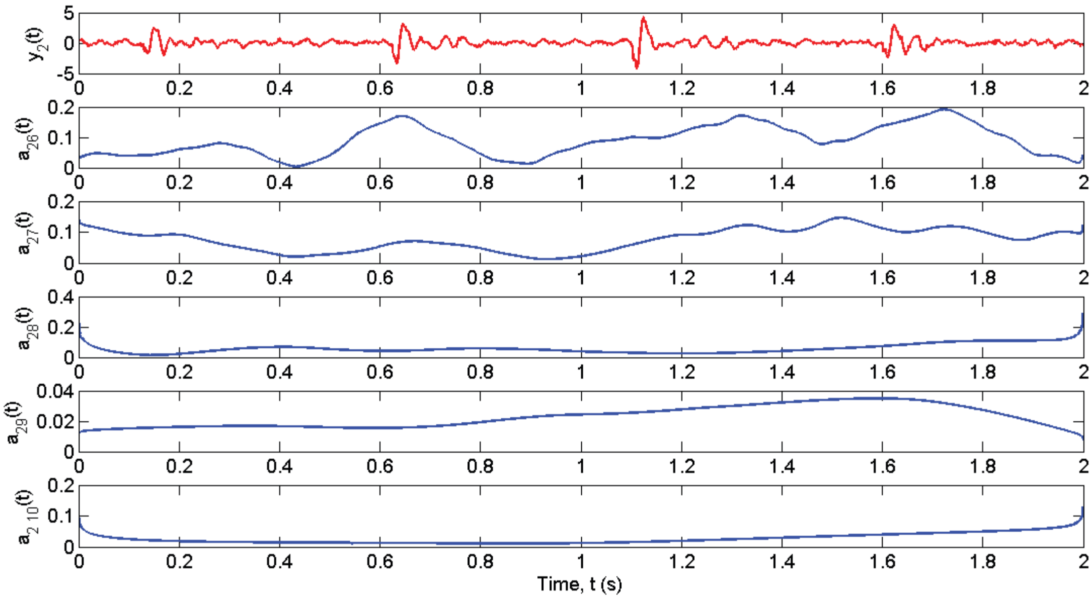

Figure 6. A two second output of the EMD block. The red curve shows the original data. The blue curves represent the amplitude signal of the final five modes.(for color image see electronic version of manuscript)

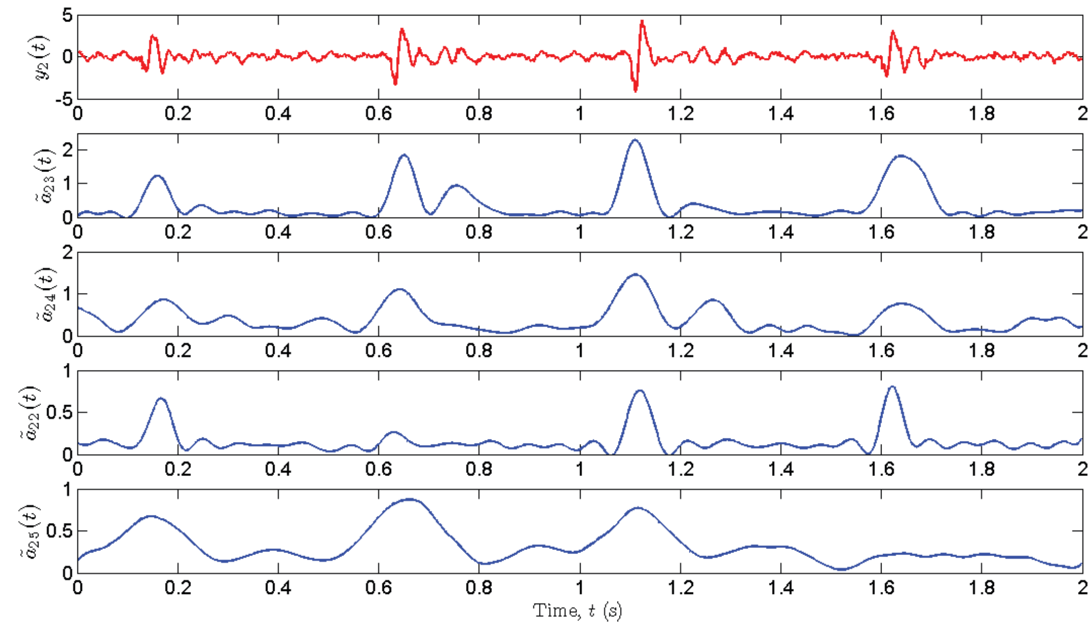

Figure 7. Output of the FDA block after mode selection. The total variation based scheme has selected, for this case, modes 3, 4, 2, 5. Mode indices are in the decreasing order of amplitude variation.(for color image see electronic version)

the *point* level oscillations as opposed to wavelets which rely on weighted averages of varying length windows. It therefore achieves much better time-scale resolution. An intrinsic mode function (IMF) of $y_i(t)$, denoted by $c_i(t)$, must satisfy two conditions,

- The number of extrema or zero-crossing must be equal or differ by one.
- At any point, the mean values of the envelopes defined by the local extrema is zero.

The Hilbert transform exists for all L^p classes of signals and the two points above ensure that an IMF has a well-behaved Hilbert transform. Denoting by $C_i(t)$, the Hilbert transform of $c_i(t)$, an analytic signal, $\zeta_i(t)$, can now be defined as,

$$\zeta_i(t) = c_i(t) + jC_i(t) = a_i(t)e^{j\theta_i(t)} \tag{2}$$

In the above equations, $j = \sqrt{-1}$, $a_i(t) = \sqrt{c_i(t) + C_i(t)}$ represents the instantaneous amplitude and the instantaneous phase is given by $\theta_i(t) = \arctan\left(C_i(t)/c_i(t)\right)$.

We now describe the decomposition algorithm, i.e., the process of extracting the IMFs. The decomposition method, also called sifting, uses the envelopes defined by the local extrema. The local maxima of the signal $y_i(t)$ ($t \in \mathcal{T}_r$ for each r) are connected by a cubic spline and represent the upper envelope. The lower envelope is similarly obtained by using a cubic spline to connect all the local minima. The upper and lower envelopes should cover all the data between them. Designating $m_{i1}(t)$ as the pointwise mean of the two envelopes,

$$h_{i1}(t) = y_i(t) - m_{i1}(t) \tag{3}$$

gives the first component. If $h_{i1}(t)$ is an IMF the analysis procedure is halted. However, in most cases there are undershoots and overshoots causing a non-zero local mean. The process is continued iteratively: we treat $h_{i1}(t)$ as the data, bound it by the upper and lower spline envelopes to give,

$$h_{i11}(t) = h_{i1}(t) - m_{i11}(t) \tag{4}$$

where $m_{i11}(t)$ is the mean of the lower and upper envelopes of h_{i1}. The qth iteration of the sifting process is then given by,

$$h_{i1}^{q}(t) = h_{i1}^{q-1}(t) - m_{i1}^{q}(t) \equiv c_{i1}(t) \tag{5}$$

If $h_1^q(t)$ satisfies the definition of an IMF, it is designated as $c_{i1}(t)$, the first IMF component from the data. The standard deviation between 2 successive sifting iterations is used as a stopping criterion so that the process does not continue indefinitely. In this manner $c_{i1}(t)$ contains the finest scale of the signal. The first residual $r_{i1}(t)$ is then given by,

$$r_{i1}(t) = y_i(t) - c_{i1}(t) \tag{6}$$

We now treat $r_1(t)$ as the data subject it to the sifting process as described above. This gives us L IMFs, $c_{i1}(t), c_{i2}(t), \ldots, c_{il}(t), \ldots, c_{iL}(t)$. The sifting process is stopped when either of the following conditions are true: (i) $|c_{iL}(t)| < \varepsilon$, or $|r_{iL}| < \varepsilon$ for a pre-specified $\varepsilon > 0$, or, (ii) r_{iL} is a monotone function or constant. Huang et al.[11] state that the IMFs are orthogonal in most practical situations, however, it cannot be guaranteed in theory. The decomposition can be finally expressed as,

$$\begin{aligned} y_i(t) &= \sum_{l=1}^{L} c_{il}(t) + r_{iL} \\ &\approx \sum_{l=1}^{L} c_{il}(t) \end{aligned} \tag{7}$$

The analytic signal for each IMF can be calculated as in (2) so that,

$$\zeta_{il}(t) = a_{il}(t)\exp(j\theta_{il}(t)) \tag{8}$$

EMD decomposes the given signal into its constituent oscillation modes, and the instantaneous amplitude, $a_{il}(t)$, of the analytic signal characterizes the envelope of each oscillation mode. Since EMD is data-driven, adaptive and is based on the local characteristic time scale of the data it is suitable for nonstationary and nonlinear processes. This is in stark contrast to the Fourier and wavelet based feature sets that require stationarity and linearity as necessary conditions for analysis.

4.2 Functional Data Analysis

In the functional data analysis (FDA) framework, we assume that observations are made from a continuous family of curves. Functional data analysis also has the advantage that it does not make assumptions on stationarity or low dimensionality. The following paragraphs provide a brief description of the theory as applied to the analytic signal after EMD. More details may be found in the literature.[12, 13]

In order to smooth $a_{il}(t)$, we express it as a linear combination of B-spline basis functions. A variety of basis functions are known in numerical analysis literature.[14] B-splines are appropriate for our application because of their smoothness properties. A B-spline of degree 6 ensures that the second derivative of the signal is smooth.[12] A footstep is a signal of impulsive nature. In other words, it is characterized by a sharp onset. In order to faithfully follow a sharp transition, a large number of basis functions is required.

Let P be the number of bases. Denote the basis functions by $\{\varphi_p(t)\}_{1\leq p\leq P}$ and the coefficients by $b_{p,il}$. Note that these coefficients will have to be estimated for all modes, l, of each sensor i. For notational simplicity we drop the subscript 'il' and refer to $b_{p,il}$ as b_p. We can represent the P-dimensional basis function vector $\boldsymbol{\varphi}(t)$ as a $|\mathcal{T}_r| \times P$ matrix, $\mathbf{\Phi}$.We estimate $\mathbf{b}$, the vector of coefficients b_p, by minimizing the weighted sum of least squares,

$$f_{WMSSE} = (\mathbf{a}_{il} - \mathbf{\Phi}\mathbf{b})^{\mathrm{T}}\mathbf{W}(\mathbf{a}_{il} - \mathbf{\Phi}\mathbf{b}) \tag{9}$$

where $\mathbf{a}_{il}$ is a vector, each element of which is $a_{il}(t)$ for every $t \in \mathcal{T}_r$ and $\mathbf{W}$ is a positive semidefinite matrix that allows for unequal weighting and is typically taken to be the inverse of the covariance matrix of the background process.

Solving for (9) may involve the inversion of ill-conditioned matrices. In order to regularize an ill-conditioned weighted least squares cost function, Ramsay and Silverman[12] define a metric that penalizes the roughness of a function $x(t)$,

$$\mathrm{PEN}_2(x) \triangleq \int [\ddot{x}(t)]^2 dt \tag{10}$$

where $\ddot{x}(t)$ is the second time derivative of $x(t)$. The integrand in the above equation is a measure of the curvature of x at t. Denote the time sequence t as the vector $\mathbf{t}$. Noting that $\mathbf{\Phi}\mathbf{b} = x(\mathbf{t})$, the roughness penalty based least squares fit is then expressed as the minimization of,

$$f_{PMSSE} = (\mathbf{a}_{il} - x(\mathbf{t}))^{\mathrm{T}}\mathbf{W}(\mathbf{a}_{il} - x(\mathbf{t})) + \lambda \times \mathrm{PEN}_2(x) \tag{11}$$

Let $\tilde{\mathbf{b}}$ be the optimal estimate of $\mathbf{b}$ obtained by minimizing (11). Then even for the limiting case of $\lambda \to 0$, $\tilde{a}_{il}(t) = \sum_p \varphi_p(t)\tilde{b}_p$ is the smoothest twice-differentiable curve that exactly fits the data. In practice, λ must be sufficiently small to allow for stability of the numerical optimization. For our application, we used $\lambda = 10^{-6}$.

4.3 Selection of modes

Under the assumption of a reasonable SNR, we seek to identify modes with significant *variation* in their amplitude. This would correspond to the footfalls that modulate the sensor output. We emphasize the term "amplitude variation" since a mode, $\tilde{a}_{il}(t)$, of constant amplitude, may have a large norm, $\|\tilde{a}_{il}(t)\|_1$, and yet not convey any information about the presence of footsteps. In order to retain only those modes (or components) that contain footstep information, we propose the use of the total variation norm as a metric to determine which modes contain this information. The total variation norm (TV) of a real function $f(s), s \in [a, b]$ is defined as,[15]

$$\mathrm{TV}[f] \triangleq \sup_P \sum_{i=1}^{n_P} |f(s_i) - f(s_{i-1})| \tag{12}$$

where the supremum runs over the set of all partitions $a = s_0 < s_1 < \cdots < s_{n_P} = b$ of the interval $[a, b]$ and $n_P \in \mathbb{N}$. If $f(s)$ is differentiable in $[a, b]$ (12) can be expressed as,[16]

$$\mathrm{TV}[f] = \int_a^b |f'(s)| ds \tag{13}$$

The TV norm of a function enhances the information contained in sharp rises in signal amplitude. It has been used as a regularizing term to achieve edge preserving smoothing in image processing applications.[17] The instantaneous amplitude of footsteps also have a sharp onset; this is the information that we wish to emphasize through the use of TV. Therefore, the total variation of $\tilde{a}_{il}(t)$ is given by,

$$T_l^i = \mathrm{TV}[\tilde{a}_{il}] = \int_{t \in \mathcal{T}_r} \left| \frac{d}{dt} \tilde{a}_{il}(t) \right| dt \tag{14}$$

We denote the ordered TV norms as $T_{(l)}^i$ $(l = 1, 2, \ldots, L)$ so that $\min\{T_1^i, T_2^i, \ldots, T_L^i\} = T_{(1)}^i \leq T_{(2)}^i \leq \cdots \leq T_{(l)}^i \leq \cdots \leq T_{(L)}^i = \max\{T_1^i, T_2^i, \ldots, T_L^i\}$. We choose only those modes corresponding to $T_{(l)}^i$, $l = L, L-1, \ldots, L-M+1$, that satisfy,

$$\frac{1}{S_T} \sum_{l=L}^{L-M+2} T_{(l)}^i < 0.9 \leq \frac{1}{S_T} \sum_{l=L}^{L-M+1} T_{(l)}^i, \tag{15}$$

where,

$$M \leq L \quad \text{and} \quad S_T = \sum_{\text{all } l} T_{(l)}^i$$

Note that the summation in (15) decrements through the index l starting with $l = L$.

What remains, now, is for the instantaneous amplitudes across the selected modes need to be combined in a meaningful way. Since we are interested in a detector whose test statistic is signal energy (refer Section 5), we cannot simply add the energies of the individual modes because the instantaneous amplitudes across the different modes are not orthogonal. Denote by M the number of selected modes and by $\tilde{\mathbf{a}}_i$ the $M \times |\mathcal{T}_r|$ matrix where each entry in the matrix is the scalar $\tilde{a}_{il}(t), t \in \mathcal{T}_r$. We now perform PCA on the M variate amplitude vector of $|\mathcal{T}_r|$ observations. From the M resultant scores only the first principal score, denoted by $z_i(t)$, is retained and is input to the subsequent energy detector (Fig. 4). Thus we achieve a further reduction in signal dimensionality from $M \times |\mathcal{T}_r|$ to $1 \times |\mathcal{T}_r|$.

5. RESULTS

An energy detector for each frame can be implemented as a test of variance of $z_i(t)$, $\sigma_{z_i}^2$,

$$S^2 = \widehat{\sigma_{z_i}^2} \underset{H_0}{\overset{H_1}{\gtrless}} \eta_\alpha \tag{16}$$

where H_0 denotes the background process and H_1 denotes the alternative hypothesis of the presence of footsteps. The sample estimate of variance is denoted by $\widehat{\sigma_{z_i}^2}$ and the threshold η_α is selected to constrain the probability of false alarm (P_{FA}) to a pre-specified level α. Figure 8 shows the receiver operating characteristic (ROC) for the detector. The curve represents the average over all trials and sensors. We also compare the detector ROC to the case when EMD-FDA based signal processing is not applied (i.e., $z_i(t) = y_i(t)$). As evident from Fig. 8, our signal processing scheme results in an improvement of approximately 16% at $\alpha = 0.05$.

Note that η_α can be obtained only if the distribution under H_0 is known. A bootstrap based test[18] provides a non-parametric approach to threshold selection under the α constraint. We used a non-pivotal bootstrap test and set α to 0.05. We also considered the case of fusing individual sensor decisions using the majority rule.[19] These results are summarized in Table 2.

An interesting observation is that the probability of false alarm for the unprocessed signal (raw data), using the bootstrap test, is much higher than 0.05 although the test is a level $\alpha = 0.05$ test. We conjecture that this may be because of non-zero correlation in the time series, however this needs further study. The results after majority fusion show that the probability of detection achieved by the EMD-FDA processed signal is slightly lower than that of the raw signal case, and is achieved at a significantly lower global false alarm of 0.0127.

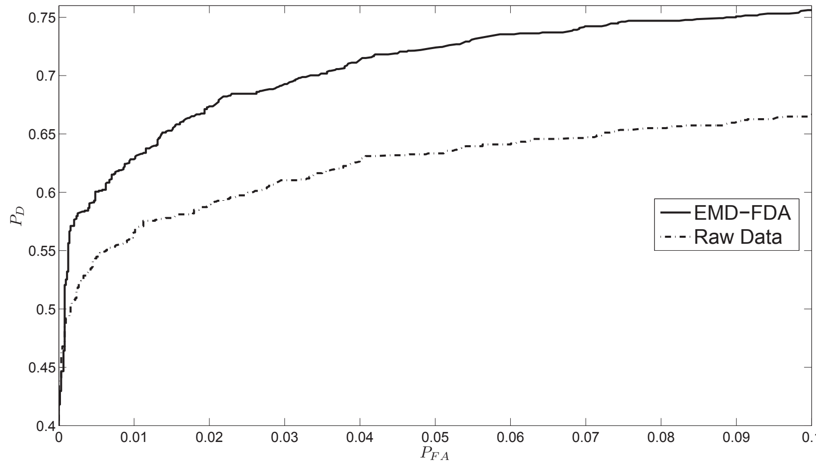

Figure 8. Receiver operating characteristic (ROC) comparing detector performance

Table 2. Results for bootstrap detection, $\alpha = 0.05$

Sensor	*Raw Data*		*EMD-FDA*	
i	P_{FA}	P_D	P_{FA}	P_D
1	0.2712	0.7361	0.0508	0.6528
2	0.1525	0.9167	0.0339	0.6713
3	0.1271	0.7963	0.0890	0.6852
4	0.3263	0.8287	0.1102	0.8194
5	0.3390	0.8148	0.0593	0.7778
6	0.4195	0.8796	0.0805	0.8380
	Fusion (Majority Rule)			
	0.2500	0.8889	0.0127	0.8380

6. CONCLUSION

In this paper, we proposed a data-driven signal processing scheme for footstep detection. We presented an analysis of experimental data collected at Syracuse University and showed that the data exhibits significant nonlinearity and nonstationarity. We used a detector based on unprocessed data as a benchmark and showed that our detector is able to achieve significant improvements. This signal processing scheme, in principle, can also be used with acoustic sensors. EMD is able to decompose the signal in terms of oscillation modes present in the signal. This means that the amplitude of the analytic function of one or more modes will carry the footstep envelope information. Future work will focus on improving detection performance by fusing information obtained using heterogeneous modalities.

ACKNOWLEDGMENTS

Research was sponsored by Army Research Laboratory and was accomplished under Cooperative Agreement No. W911NF-07-2-0007. It was also supported in part by ARO grant W911NF-06-1-0250. The views and conclusions contained in this document are those of the authors and should not be interpreted as representing the official policies, either expressed or implied of the Army Research Laboratory or the U.S. Government. The U.S. Government is authorized to reproduce and distribute reprints for Government purposes notwithstanding any copyright notation hereon.

REFERENCES

1. R. E. Bland, "Acoustic and seismic signal processing for footsetp detection," Master's thesis, Massachusetts Institute of Technology, Dept. of Electrical Engineering and Computer Science, 2006.
2. G. Succi, D. Clapp, R. Gampert, and G. Prado, "Footstep detection and tracking," in *Proc. SPIE - Int. Soc. Opt. Eng. (USA)*, **4393**, pp. 22 – 9, (USA), 2001.
3. H.-F. Xing, F. Li, and Y.-L. Liu, "Wavelet denoising and feature extraction of seismic signal for footstep detection," in *Proceedings of the 2007 International Conference on Wavelet Analysis and Pattern Recognition, ICWAPR '07*, **1**, pp. 218 – 223, (Piscataway, NJ 08855-1331, United States), 2008.
4. A. A. Dibazar, H. O. Park, and T. W. Berger, "The application of dynamic synapse neural networks on footstep and vehicle recognition," in *Proc. International Joint Conference on Neural Networks IJCNN 2007*, pp. 1842–1846, 12–17 Aug. 2007.
5. K. M. Houston and D. P. McGaffigan, "Spectrum analysis techniques for personnel detection using seismic sensors," in *Unattended Ground Sensor Technologies and Applications V*, E. M. Carapezza, ed., **5090**(1), pp. 162–173, SPIE, 2003.
6. S. G. Iyengar, P. K. Varshney, and T. Damarla, "On the detection of footsteps based on acoustic and seismic sensing," in *Conference Record of the Forty-First Asilomar Conference on Signals, Systems and Computers ACSSC 2007*, pp. 2248–2252, 4–7 Nov. 2007.
7. J. S. Bendat and A. G. Piersol, *Random Data: Analysis and Measurement Procedures*, John Wiley & Sons, Inc., New York, NY, USA, 1990.
8. Geo Space, LP, "Charts for GS-20DX & GS-20DM." Accessed online, March 2009. `http://www.geospacelp.com/c_20dx.shtml`.
9. T. Schreiber and A. Schmitz, "Surrogate time series," *Physica D* **142**(3), pp. 346–382, 2000.
10. J. Theiler, S. Eubank, A. Longtin, B. Galdrikian, and J. D. Farmer, "Testing for nonlinearity in time series: the method of surrogate data," in *Conference proceedings on Interpretation of time series from nonlinear mechanical systems*, pp. 77–94, Elsevier North-Holland, Inc., (New York, NY, USA), 1992.
11. N. E. Huang, Z. Shen, S. R. Long, M. C. Wu, H. H. Shih, Q. Zheng, N.-C. Yen, C. C. Tung, and H. H. Liu, "The empirical mode decomposition and the Hilbert spectrum for nonlinear and non-stationary time series analysis," *Proceedings of the Royal Society A: Mathematical, Physical and Engineering Sciences* **454**(1971), pp. 903–995, 1998.
12. J. O. Ramsay and B. W. Silverman, *Functional Data Analysis*, Springer Series in Statistics, Springer, June 2005.
13. F. Ferraty and P. Vieu, *Nonparametric Functional Data Analysis: Theory and Practice (Springer Series in Statistics)*, Springer, 1 ed., June 2006.
14. W. Cheney and D. Kincaid, *Numerical Mathematics and Computing*, International Thomson Publishing, 1998.
15. E. Kreyszig, *Introductory Functional Analysis with Applications*, Wiley, 1 ed., 1989.
16. D. M. Strong and T. F. Chan, "Exact solutions to total variation regularization problems," UCLA CAM Report, University of California, LA, 1996.
17. T. Chan and J. Shen, *Image Processing And Analysis: Variational, Pde, Wavelet, And Stochastic Methods*, Society for Industrial and Applied Mathematics, Philadelphia, PA, USA, 2005.
18. A. M. Zoubir and D. R. Iskander, *Bootstrap techniques for signal processing*, Cambridge University Press, Cambridge, U.K., 2004.
19. P. K. Varshney, *Distributed Detection and Data Fusion*, Springer-Verlag New York, Inc., Secaucus, NJ, USA, 1996.